Design and comparison of different RST controllers for PMSM control

M.Khanchoul, M.Hilairet
Laboratoire de Génie Electrique de Paris (LGEP)/ SPEE-Labs
CNRS UMR8507, SUPELEC, Université Pierre et Marie Curie P6, Université Paris-Sud 11
11, rue Joliot Curie, Plateau de Moulon - F91192 Gif Sur Yvette Cedex
Email: (mohamed.khanchoul,mickael.hilairet)@lgep.supelec.fr

***Abstract*—Pollution problems have led the industry to seek solutions for the development of electric vehicle technology. Therefor the conventional compressors are substituted by electric compressor. In this paper, two RST controllers are proposed and compared for driving the compressor.**

I. Introduction

Nowadays, the automotive industry is facing two major drawbacks: gas emission due to conventional vehicle and energy consumption. Recently, all car manufacturers are focusing on electric vehicle technology to address these problems. However, this technology will face to major drawback, the sensitivity of the battery autonomy to climatic condition. In hard weather conditions the battery autonomy is reduced to $100\,\text{km}$ on even less depending on the severity of weather condition, where as a rang of $150 - 200\,\text{km}$ could be obtained in normal condition. Moreover, in order to ensure thermal comfort in the vehicle, regular air compressor needs to be replaced by electric air compressor. Thus, electric air compressor provides the thermal comfort in the vehicle and furthermore preserves the battery autonomy.

The electric compressor is composed of three parts: the power electronics, the scroll and the electrical motor. The power electronics system is used to control the mechanical speed of the motor and thus the flow of the cooling gas. Due to heat exchange which occurs in the electric compressor, many parameters of the motor such as the inductances and resistances can change, especially at the start-up of the motor. Therefore, it is necessary to design a controller that is robust against parameter variations.

In this paper, the motor structure used is a surface mounted permanent magnet synchronous motor. This kind of motor is used due to its high efficiency, compactness structure, rapid dynamic response, high torque-to-inertia ratio, simple modeling and control.

In this work, the PMSM is controled by a regular Field Oriented Control based on digital RST controllers. The RST controller has some attractive features: it can independently manage the dynamic tracking and disturbance rejection dynamics, it can take into account the delay in the process, etc. In the state of the art, there are two methods for designing the RST controller: regular RST controller proposed in [1]-[7] and specific RST controllers designing for system with sinusoidal or ramp references [8]- [10].

The RST controller for sinusoidal references is well suited for power electronics applications, as inverters. This controller ensures zero steady state error with a sinusoidal references, and thus brings a high precision. For speed control of electrical motors, regular RST controllers or RST for ramp references is often preferred, because the speed reference trajectory are generally constant or a ramp.

In this paper, the performances of the regular RST controller and RST for ramp references are compared. The precision, robustness and sensitivity are analysis.

This paper is organized as the following: the second part is dedicated to present the controllers design. The third part is devoted to the speed and current controllers design of the PMSM. The comparison and discussion on the performance (precision, robustness and sensitivity) are detailed in this latter section.

II. Controllers design

The RST controller as its name suggests is a polynomial structure. It consists of three polynomials R, S and T. The controller design is based on a robust pole placement.

A. Design of the regular RST

Considering a process and a controller described by polynomials according to the diagram described in Fig. 1, where $\frac{B(z^{-1})}{A(z^{-1})}$ represents the open-loop transfer function. Thus, the closed-loop is given by:

$$\begin{aligned} y &= \frac{B(z^{-1})T(z^{-1})}{A(z^{-1})S(z^{-1}) + B(z^{-1})R(z^{-1})} y_{ref} \\ &+ \frac{S(z^{-1})}{A(z^{-1})S(z^{-1}) + B(z^{-1})R(z^{-1})} d \end{aligned} \quad (1)$$

where y is the output, y_{ref} is the reference and d represents a disturbance. $R(z^{-1})$, $S(z^{-1})$ are polynomials and solution of the Diophantine equation (also called Bezout equation) obtained by a robust pole placement strategy. The Diophantine equation is given as follows:

$$A(z^{-1})S(z^{-1}) + B(z^{-1})R(z^{-1}) = D(z^{-1}) \quad (2)$$

Two conditions must be satisfied: i.e. $T(1) = R(1)$ to obtain unitary static gain and $S(1) = 0$ in order to reject the disturbance in steady state. In addition, the degree of $T(z^{-1})$

978-1-61284-972-0/11/$26.00 ©2011 IEEE

is a parameter that is defined by the designer. It can be used to simplify tracking transfer $\frac{y}{y_{ref}} = \frac{BT}{D}$.

In this paper, a strictly proper controller is used in each case. The controller has the following properties:

- deg(S)=deg(A)+1
- deg(R)=deg(A)
- deg(D)=deg(R)+deg(S)

Assuming a first order system given as follow:

$$G_{ol}(p) = \frac{K}{p + p_1} \tag{3}$$

The discrete time representation of the plant presented in (3) is:

$$G_{ol} = \frac{K_1(1 - z_1)z^{-1}}{1 - z_1 z^{-1}} \tag{4}$$

where $z_1 = e^{-p_1 T_e}$, $K_1 = \frac{K}{p_1}$ and T_e is a sampled period. Since $deg(A)$ is equal to one:

$$R(z^{-1}) = r_0 + r_1 z^{-1} \tag{5}$$
$$S(z^{-1}) = (1 - z^{-1})(s'_0 + s'_1 z^{-1}) \tag{6}$$

Then the poles of the closed-loop are imposed in the discrete plan, such as:

$$z_{1,2} = e^{(-\xi\omega_0 \pm j\omega_0\sqrt{1-\xi})T_e} \tag{7}$$
$$z_3 = e^{-\omega_0 T_e} \tag{8}$$

that leads to the polynomial $D(z^{-1})$:

$$D(z^{-1}) = (1 - z_1 z^{-1})(1 - z_2 z^{-1})(1 - z_3 z^{-1}) \tag{9}$$

Therefore the coefficients of polynomials R and S are identified as follow:

$$\begin{bmatrix} 1 & 0 & 0 & 0 \\ -(1+z_1) & 1 & K_1(1+z_1) & 0 \\ z_1 & -(1+z_1) & 0 & K_1(1+z_1) \\ 0 & z_1 & 0 & 0 \end{bmatrix} \times \begin{bmatrix} s'_0 \\ s'_1 \\ r_0 \\ r_1 \end{bmatrix} = \begin{bmatrix} d_0 \\ d_1 \\ d_2 \\ d_3 \end{bmatrix} \tag{10}$$

where d_0, d_1, d_2, d_3 represents the coefficients of Diophantine equation obtained after the development of the equation (9).

To protect the components of each system, the controller output is saturated. Therefor, a saturation associated with an anti-windup is implemented, as shown on Fig. 2.

As mentioned previously, the polynomial T is a free tuning parameter. It is defined as follows:

$$T(z^{-1}) = \frac{R(1)}{F(1)} F(z^{-1}) \tag{11}$$

where F is a filter that contains the poles chosen for compensation in order to specify or to impose the desired closed-loop poles.

B. Design of RST for ramp references

This type of controller is the same as detailed previously but the difference is in the determination of a polynomial B_m of the closed-loop, and thus in the definition of T. In this case, the determination of the polynomial T is a free tuning parameter that allows to cancel the steady state error during transient [8]. The closed-loop transfer function is specified as follows:

$$G_{cl} = F_m(z^{-1}) = \frac{B_m(z^{-1})}{A_m(z^{-1})} \tag{12}$$

The transfer function can be decomposed as follow:

$$G_{cl} = \frac{B^+(z^{-1})B^-(z^{-1})}{A^+(z^{-1})A^-(z^{-1})} \tag{13}$$

where B^- and A^- contain all poles and zeros of $G_{cl}(z^{-1})$ that can not be compensated. B^+ and A^+ contain all the other terms. In our case, A^-, A^+, B^- and B^+ are defined as follows:

$$A^- = 1 - z_1 z^{-1} \tag{14}$$
$$A^+ = 1 \tag{15}$$
$$B^- = z^{-1} \tag{16}$$
$$B^+ = K_1(1 - z_1) \tag{17}$$

The closed-loop transfer function is defined as:

$$G_{cl} = F_m(z^{-1}) = \frac{BT}{AS + BR} \tag{18}$$

then, the equality between Equ. 12 and Equ. 18 must be performed. $F_m(z^{-1})$ is chosen arbitrarily in order to impose the desired closed-loop poles. But with the constraint that

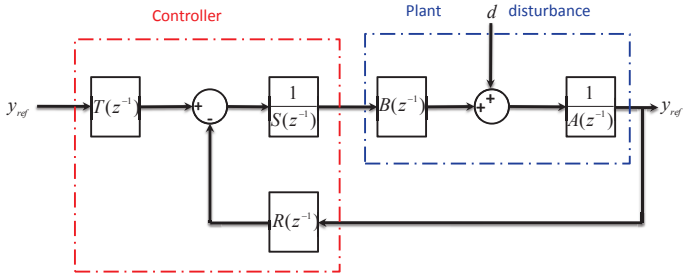

Figure 1. Plant with RST structure

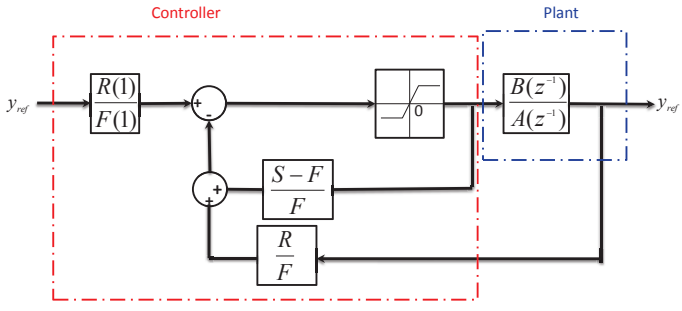

Figure 2. RST structure with an antiwindup action.

$B_m(z^{-1})$ has to contain as a factor the system plant pure delay, its uncompensable zeros and zeros that the designer decides not to compensate, i.e. $B^-(z^{-1})$:

$$B_m = B^{-1}B_m^{'} \tag{19}$$

According to Equ. 12, the partial transfer function from reference y_{ref} to error signal $\epsilon = y_{ref} - y$ is given by:

$$\frac{\epsilon(z^{-1})}{y_{ref}(z^{-1})} = \frac{A_m - B_m}{A_m} \tag{20}$$

In order to cancel steady state errors in response to a ramp reference $y_{ref}(t) = \alpha t^m$, with the corresponding Z transform:

$$y_{ref}(z^{-1}) = \frac{y_1^*}{(1-z^{-1})^2} \tag{21}$$

where y_1^* is a polynomial in z^{-1}. It is necessary and sufficient that $(1-z^{-1})^2$ divides $A_m - B_m$; the following equation must be solved:

$$A_m - B_m = (1-z^{-1})^2 L(z^{-1}) \tag{22}$$

This equation is called auxiliary Diophantine equation in [9]. $L(z^{-1})$ is an unknown polynomial to determined, and its order is a tuning parameter. The closed-loop system is a second order:

$$A_m = 1 - 2e^{-\xi\omega_0 T_s} cos(\omega_p T_s) z^{-1} + e^{-\xi\omega_0 T_s} z^{-2} \tag{23}$$

with $\omega_p = \sqrt{1-\xi^2}$. Polynomials $L(z^{-1})$ and $B_m^{'}(z^{-1})$ become solutions to Equ. 22, and tuning parameters $L(z^{-1})$ and $B_m^{'}$ are defined as:

$$L(z^{-1}) = l_0 + l_1 z^{-1} \tag{24}$$

$$B_m^{'}(z^{-1}) = b_0^{'} + b_1^{'} z^{-1} \tag{25}$$

The resolution of Equ. 22 gives:

$$b_0^{'} = 2e^{-\xi\omega_0 T_s} cos(\omega_p T_s) - 2 \tag{26}$$

$$b_1^{'} = e^{-\xi\omega_0 T_s} - 1 \tag{27}$$

$$l_0 = 1 \tag{28}$$

$$l_1 = 0 \tag{29}$$

Moreover, another constraint is imposed in order to ensure a unity gain in steady state. A constant factor A_0 is introduced to make $F_m(1) = 1$, i.e.:

$$T = A_0 B_m^{'} \tag{30}$$

where the filter polynomial A_0 is often set equal to one [9]. From Eq. 22, polynomials L and $B_m^{'}$ are identified, so polynomial T is known. The determination of polynomial R and S defined in the previous section are still available.

III. Permanent Magnet Synchronous Motor Control via RST controllers

A. Motor model

The control structure of the PMSM is a regular Field Oriented Control, as shown in Fig.3.

The model of the synchronous machine is defined in the (dq) coordinate and is given as follows:

$$\begin{aligned} L_d \tfrac{di_d}{dt} &= -R_s i_d + \omega L_q i_q + v_d \\ L_q \tfrac{di_q}{dt} &= -R_s i_q - \omega L_d i_d - \omega\phi + v_q \\ J\tfrac{d\Omega}{dt} &= P\left(L_d - L_q\right) i_d i_q + P\phi i_q - f\Omega \end{aligned} \tag{31}$$

In these equations, P is the number of pole pairs, v_d, v_q, i_d, i_q are voltages and currents in the (dq) coordinate, L_d and L_q are the stator inductances which are equal in the case of cylindrical rotor, R_s is the stator winding resistance, f is viscous friction coefficient, ϕ and J are the flux produced by the permanent magnets and the moment of inertia respectively. The angular velocity ω is measured in electrical radians per second (the connection between electrical and mechanical variables is simply $\omega = P\Omega$). $e_d = \omega L_q i_q$ and $e_q = -\omega L_d i_d - \omega\phi$ represents the terms of coupling. these terms are compensated after design the controllers.

According to the equations presented above, the transfer functions of the two electrical subsystems are given as follows:

$$\frac{i_d}{v_d} = \frac{\frac{1}{L_d}}{p + \frac{R_s}{L_d}} \tag{32}$$

$$\frac{i_q}{v_q} = \frac{\frac{1}{L_q}}{p + \frac{R_s}{L_q}} \tag{33}$$

and the transfer function of the mechanical subsystem is:

$$\frac{\Omega}{i_q} = \frac{\frac{P\phi}{J}}{p + \frac{f}{J}} \tag{34}$$

According to the transfer functions mentioned in Equa. 33-34 and Equa. 3, the regular RST and RST with ramp reference can be designed.

B. Simulation result

This section is composed of 3 parts: firstly, nominal test are performed, where the two RST controllers are compared versus speed and the current along the axis q. The second part is dedicated to robustness tests and the third part is devoted to sensitivity tests.

1) Nominal tests: Figs. 4-7 present the speed control, the current control in the q axis, the error between the reference and measurement for both speed and current control. The simulation results show that the RST controller with ramp reference exhibit a good precision versus the classical RST controller. We can notice that the measured speed follows perfectly the reference. However at startup, this controller has a slight disadvantage and it present also a slight overshoot.

2) Robustness tests: The robustness of the two controllers has been tested against parameters variation. Figs. 8-9 show the speed and the current control with a variation of the resistance and inductance of 50%. The simulations show that both controllers exhibit good performances.

3) Sensitivity test: In this part, the mechanical position sensor has been modeled to observe controllers behavior versus position sensor noise. Here, the position sensor resolution is

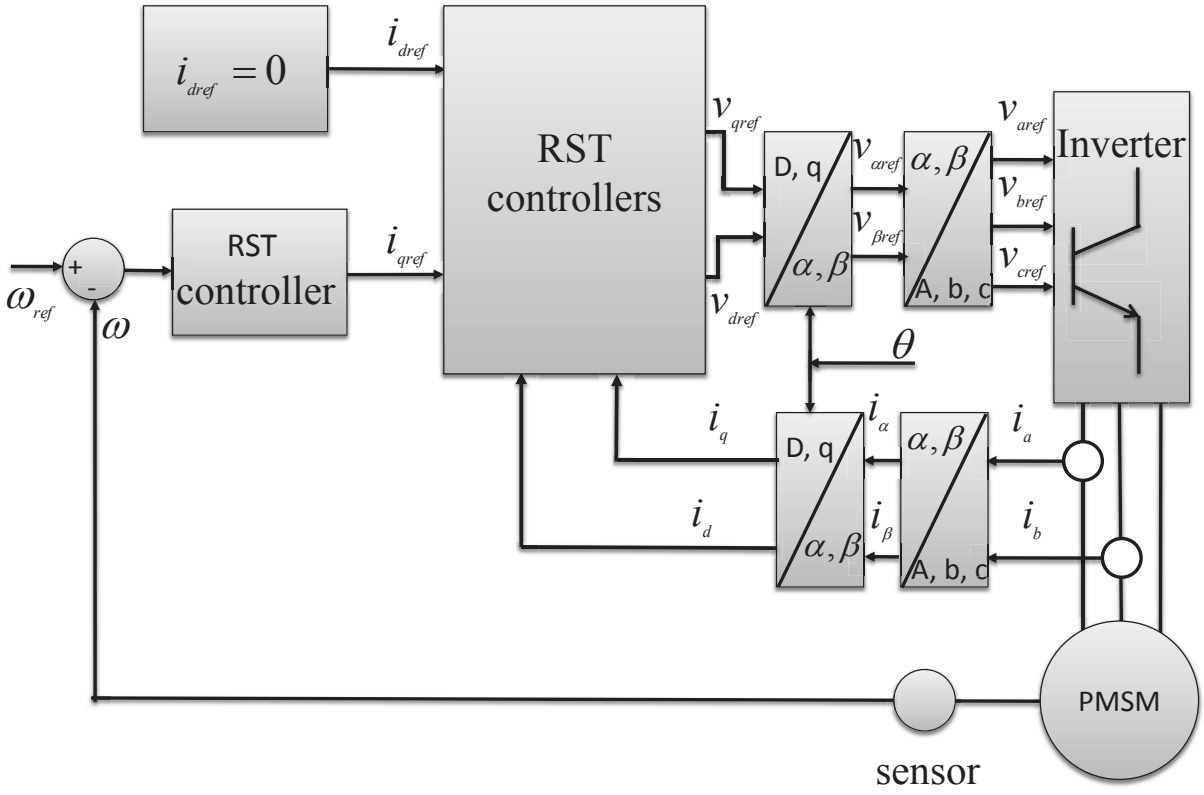

Figure 3. Control structure via RST.

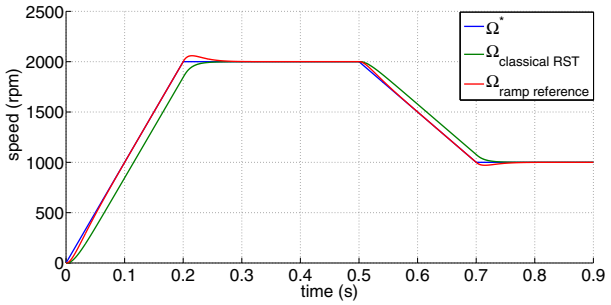

Figure 4. References and measured speed for both controllers.

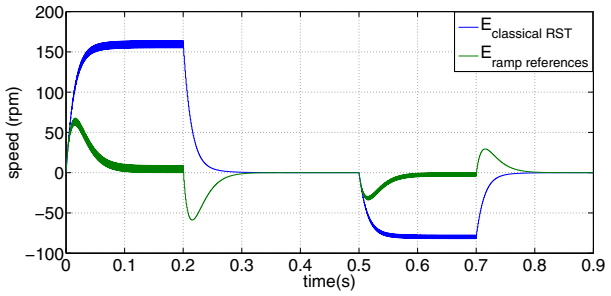

Figure 5. Error between the reference and measured speed for th two controllers.

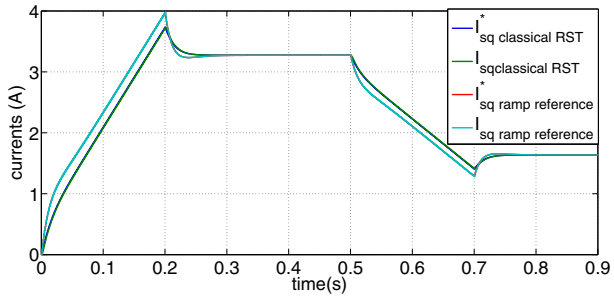

Figure 6. Current behaviour for both controllers.

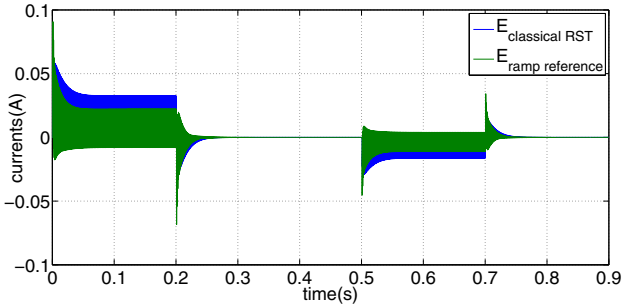

Figure 7. Error between the reference and measured current for th two controllers.

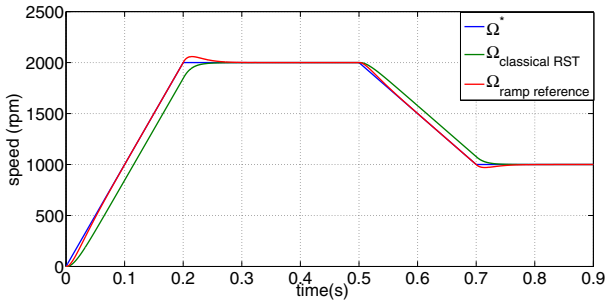

Figure 8. Behavior of speed with 50% variation in resistance and inductance of the two controllers.

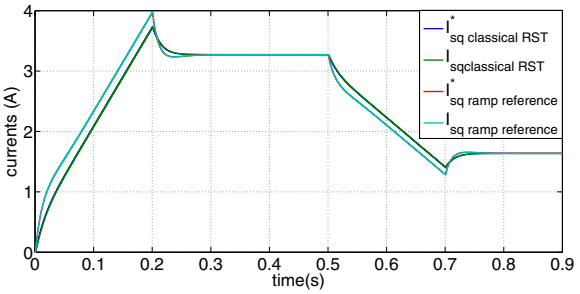

Figure 9. Behavior of current with 50% variation in resistance and inductance of both controllers.

4×3600 points per turn. Figs. 10-12 show the speed, the current control and the closed-loop gain of both controllers

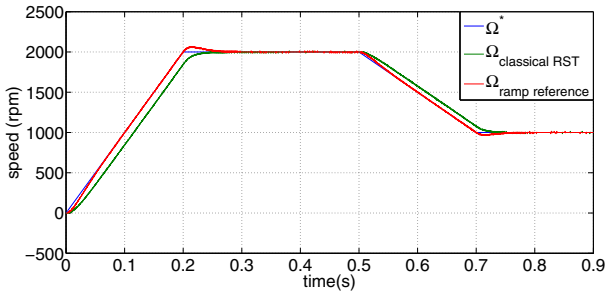

Figure 10. Behavior of speed in the presence of noise for the two controllers.

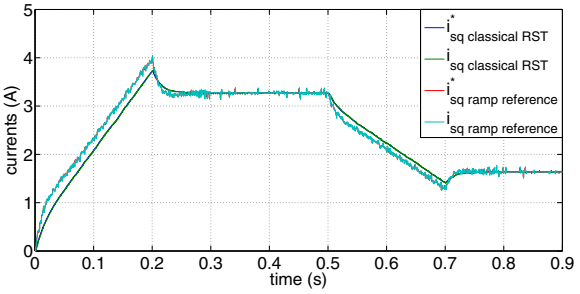

Figure 11. Behavior of current in the presence of noise for the two controllers.

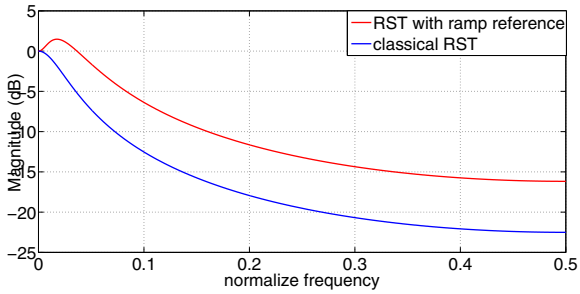

Figure 12. Frequency response of the closed-loop of the two system.

The Figs.10 show that the regular RST controller is less sensitive to the speed measurement noise due to the position sensor quantification.The Figs.11 shows more clarity on this aspect especially in transient. This observation is also validated by the frequency response of the mechanical closed-loop system. The RST with ramp reference exhibits an over-shoot.

IV. Conclusion

In this paper, the comparison between the two RST structures has been studied versus precision, robustness and sensitivity. This study proved that the RST with ramp references is better than the regular RST to cancel the steady state error with a ramp references. However, this latter is more sensible to the position sensor quantification. Therefore, it seems that complementary tests are needed based on experimentation.

Acknowledgment

This work was supported by the French automotive cluster MOVEO in a FUI program, through the project COMPACITE.

Table I
Machine parameters

Rated output power	$P_n = 6\,\text{kW}$
Rated torque	$C_n = 6\,\text{N.m}$
Rated speed	$\Omega = 10000\,\text{rpm}$
Rated voltage	$V_n = 355\,\text{V}$
Rated current	$I_n = 22.6\,\text{A}$
Stator resistance	$R_s = 0.12\,\Omega$
Stator inductance	$L = 0.0013\,\text{H}$
Rated flux	$\Phi_r = 0.04\,\text{Wb}$
Number of pole pairs	$p = 4$
Inertia load	$J = 1.0625e{-}4\,\text{Kg.m}^2$
Viscous coefficient	$f = 0,0025\,\text{N.m/s}$

References

[1] X.L. Shi, F. Morel , B. Allard,D. Tournier,J.M. Retif "A Digital-Controller Parameter-Tuning Approach, Application to a Switch-Mode Power Supply," *ISIE*, 2007

[2] M.B. Camara,H. Gualous, F. Gustin, A. Berthon,B. Dakyo "DC/DC converter design for supercapacitor and battery power management in hybrid vehicle applications polynomial control strategy," *IEEE transactions on industrial electronics*,Vol. 57, no 2, February 2010.

[3] X.L. Shi, B. Allard, D. Tournier, J.M Retif, F. Morel “Digital control strategies for switch-mode power supply,” *IECON 2006*, Vol 149, no. 2, pp. 165-172, 2002.

[4] A. Pintea, D. Popescu, P. Borne ”Robust control for wind power systems,” *18th Mediterranean Conference on Control Automation*,Morocco,Marrakech, June 23-25, 2010.

[5] R. N. Andriamalala, H. Razik,L. Baghli,F.M. Sargos “Digital Vector Control of a Six-Phase Series-Connected Two-Motor Drive,” *IECON, Industrial Electronics, 34th Annual Conference of IEEE*, pp.3084-3089, Orlando, 23 January 2009.

[6] R. N. Andriamalala, H. Razik,F.M. Sargos “Indirect-Rotor-Field-Oriented-Control of a Double-Star Induction Machine Using the RST Controller,” *IECON, Industrial Electronics, 34th Annual Conference of IEEE*, pp.3108 -3113 , Orlando, 23 janvier 2009 .

[7] F. Mekri, M. Machmoum, N. Aït-Ahmed, B. Mazari, “A comparative study of voltage controllers for series active power filter,” *Electric Power Systems Research*, vol. 80, pp. 615-626, 2010.

[8] E. Ostertag, ”Steady-state error-free RST-controller design: a double Diophantine equation approach,” *Proc. 5th European Control Conference (ECC)*, Karlsruhe, Germany, 1999

[9] E. Ostertag, E. Godoy, ”RST-controller design for sinewave references by means of an auxiliary Diophantine equation,” *Proceedings of 44th IEEE Conference on Decision and Control, and the European Control Conference*, Seville, Spain, December 2005.

[10] E. Godoy, E. Ostertag, “A complete methodology for the design of a digital control law for PWM inverters,” *10th European Conference on Power Electronics and Applications (EPE)*, Toulouse, France, 2003